2023 IEEE International Symposium on Medical Measurements and Applications (MeMeA) | 978-1-6654-9384-0/23/$31.00 ©2023 IEEE | DOI: 10.1109/MeMeA57477.2023.10171946

Body measurement estimations using 3D scanner for individuals with severe motor impairments

Cristina Nuzzi
DIMI, University of Brescia
Brescia, Italy
0000-0001-5530-6136

Marco Ghidelli
DII, University of Brescia
Brescia, Italy
0000-0001-5607-7574

Alessandro Luchetti
DII, University of Trento
Trento, Italy
0000-0003-0960-0996

Matteo Zanetti
DII, University of Trento
Trento, Italy
0000-0002-8813-215X

Francesco Crenna
DIME, University of Genova
Genova, Italy
0000-0002-4803-2082

Matteo Lancini
DSMC, University of Brescia
Brescia, Italy
0000-0002-2301-876X

***Abstract*—In biomechanics, a still unresolved question is how to estimate with enough accuracy the volume and mass of each body segment of a subject. This is important for several applications ranging from the rehabilitation of injured subjects to the study of athletic performances via the analysis of the dynamic inertia of each body segment. However, traditionally this evaluation is done by referring to anthropometric tables or by approximating the volumes using manual measurements. We propose a novel method based on the 3D reconstruction of the subject's body using the commercial low-cost camera Kinect v2. The software developed performs body segment separation in a few minutes leveraging alpha shape approximation of 3D polyhedrons to quickly compute a Montecarlo volume estimation. The procedure was evaluated on a total of 30 healthy subjects and the resulting segments' lengths and masses were compared with the literature.**

***Index Terms*—body segment parameters, measurements, anthropometry, biomechanics, body volume estimation**

I. Introduction

In biomechanics, the human body is often modeled using rigid links to simplify the estimation of kinetic properties using inverse dynamics [1]. This process, however, is greatly sensitive to the body segments' parameters used [2], in particular mass and center of mass of each body segment (BS). The direct measurement of these parameters is performed using medical imaging systems, which are usually not available for biomechanics studies. Another reliable option is using optimization techniques on specific motions performed by the subject [3], but this could only be applied to healthy subjects since the mobility required to perform the test may be excessive for injured subjects. Therefore, body segments' parameters are frequently estimated using data from the literature [4], in particular from regression equations based on cadaver studies [5], [6] or imaging [7] and the subject's height and weight. Data tables and references, however, refer to a specific population sample and sometimes not all necessary measurements are included, especially in the case of women or different groups. Unfortunately, in some cases, this introduces an excessive approximation [8], [9]. Manual measurements performed by trained personnel using a standard tape to measure segment dimensions could be used to obtain a subject-specific model, as suggested in [2]. From manual measurements, the volume estimation can be done using a truncated cones model roughly approximating the actual shape of the segment, especially in the case of shoulders, trunk, and pelvis [10]. This approach as well has limitations, since it relies on operator accuracy and is time-consuming.

Therefore, we propose a novel method for the subject's body segments' volume and mass estimation based on the acquisition and elaboration of 3D point clouds and color data, empowered by a deep learning skeletonization model. We developed a test bed purposely designed to work well with subjects with spinal cord injury and adopted a Kinect v2 camera to acquire the subject's data fast and robustly with little to no preparation steps, hence the testing procedure is quick and cost-effective. The point cloud and color frame are elaborated by a post-processing procedure that outputs the body segments' volumes and masses in a few minutes. Validation of the proposed approach was conducted by comparing the resulting data with anthropometric tables and manual measurements.

A. Related Work

In the last decade, 3D data acquisition systems have achieved a high degree of accuracy and significant growth in applications. With the 3D model generation, a wide variety of information can be obtained quickly and easily, including volume. In the medical field, the problem of human volume estimation has been well investigated and it is quite commonly exploited using the computerized axial tomography scan. This method has become common for large hospitals due to its accuracy, also suitable for subjects with motion impairments. However, this technology is typically not easily accessible due to its high cost. Another approach is based on the adoption of consumer-end 3D cameras such as Kinect. Authors of [11] acquired human profiles using Kinect v1 and reconstructed the bodies' mesh by exploiting commercial software. The

This project has received funding from the European Union's Horizon 2020 research and innovation programme, via an Open Call issued and executed under Project EUROBENCH (grant agreement N° 779963)

work in [12] describes a custom acquisition set-up made of multiple Kinects to extract person-specific body segments parameters, highlighting the high reliability of such a system. An evaluation of volume estimation techniques is given in [13] where the authors compared the results of their proposed algorithm to estimate the person's full body weight when in different scenarios: subject laying on a flat surface, standing still, and walking towards the sensor. Other approaches based on 3D imaging were proposed recently [14], but they require a full scan of the subject (front and rear surfaces), which is possible only if the subject is able to stand upright, which is sometimes impossible if motor impairments are present.

II. Proposed Methodology

A. Acquisition set-up

The system used for the acquisition includes an orthopedic bed on top of which a Kinect v2 camera is attached via a mechanical structure. The size of the bed base is 106 x 206 x 39 cm. A wooden frame is mechanically attached to the top of the bed base to ensure the lateral extension of the arms when the subject lays supine on the bed. An additional layer with a custom-made, high-density 0.1 kg/dm^3 foam mattress is placed on top of this frame. Due to its properties, it ensures low deformation and end-user comfort. The position of the Kinect, placed above the subject parallel to the bed, and the rigid structure on which it is installed ensure good measurement stability, as the relative position between the camera and the bed base does not change. Color and depth images acquired with the camera are collected, processed, and displayed on a cable-connected PC.

B. Point cloud filtering

The acquired point cloud includes elements of the bed and the background which interfere with a proper volume estimation procedure (see the left image in Fig. 1). Since the bed dimension is known, it is easy to eliminate points falling outside of it, such as the ground (which has a Z coordinate higher than the bed's) and the bed's support metallic elements that can be seen at the lateral extremities of the bed (X and Y coordinates outside the bed's limits). This step is named *coarse filtering*.

After the coarse filtering process ends, the point cloud includes only the subject's body and the bed surface (see the middle image in Fig. 1). To remove it, a planar fitting is performed resulting in the elimination of the bed's points. Moreover, by using the planar surface of the bed it is possible to correct any angular misalignment, thus transforming the subject's cloud in the reference system RF_{bed} centered in the middle of the bed (roughly corresponding to the subject's abdomen) and perfectly aligned to the three axes (see the right image in Fig. 1). This allows further processing to run smoothly since the subject now lays face up in the projected XY plane. It is worth noting that for visualization purposes the Z coordinate was reversed, so $Z = 0$ corresponds to the camera's position and negative values to the distance of the scene's points from it. This step is named *fine filtering*. The result of the whole procedure is an affine transformation matrix $R \mid t$ needed to transform a point in the new reference system RF_{bed}.

C. Body skeleton estimation

The subject's skeleton is estimated by the famous MediaPipe BlazePose deep learning model [15]. This model was chosen because is considered the state-of-the-art among skeletonization models and runs fast even on CPU-only machines. From the point cloud, it is possible to compute the original color image and corresponding depth map (both of the same resolution of 412x524 px) using the intrinsic parameters. The color image of the subject is elaborated by BlazePose and the body's keypoints (KPs) are saved in a JSON file. BlazePose outputs a total of 33 KPs, but only 13 of them are selected considering which are actually necessary to the biomechanical model. Moreover, the selected KPs are compatible with most skeletonization models, also allowing an easy comparison for future developments. Two more KPs are computed: the neck joint KP2 (midpoint of the shoulders) and the midpoint of the hips KP15. The 15 KPs are expressed in pixel coordinates and are shown in Fig. 2.

D. Biomechanical model

Since models used in biomechanics are based on a different segment definition from the ones based on pose estimators (such as in Figure 2), a conversion was performed between

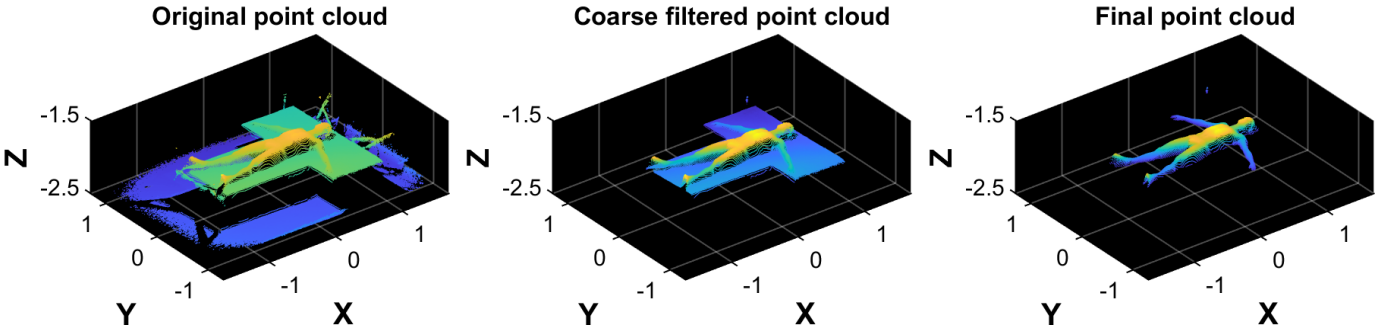

Fig. 1. Example of the point cloud filtering process. From left to right: original point cloud, result after coarse filtering (removing background), result after fine filtering (removing the test bed with planar fitting). The Z coordinate has been reversed for visualization purposes.

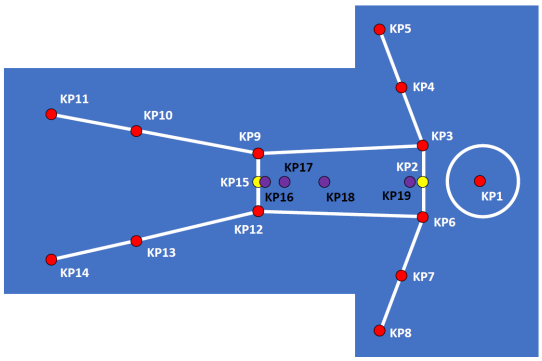

Fig. 2. Scheme of the KPs sampled from the extracted BlazePose skeleton. Red KPs correspond to BlazePose keypoints, yellow KPs are calculated as midpoints and purple KPs are computed by the biomechanical model.

the two approaches. The resulting model chosen is the one used in the Eurobench project [16], which is in turn based on the anthropometric data by [5]. From pose estimators, we have all the joints' positions related to the limbs, which could be easily translated unaltered. The head and the trunk are estimated starting from the measurement of shoulders and hips and assuming the same proportion of the spine as reported in anthropometric reference tables [5] and [6]:

1) a vector $midBody$ is computed by joining KP2 and KP15
2) the position of $C7$ (KP19) is estimated starting from the neck joint (KP2) and moving upwards of a fraction of $midBody$, estimated according to the angle between the suprasternal notch and the cervical joint center reported in [6]:

$$KP19 = KP2 + \frac{KP1 - KP2}{|KP1 - KP2|} \cdot |midBody| \cdot 17\% \quad (1)$$

3) KP17 represents the midpoint between the anterior superior iliac spines and is computed using the normative proportion of the hip reported in [5] by moving upwards KP15 (mid hip) by a fraction of the width of the hip W_{hip}:

$$KP17 = KP15 + \frac{midBody}{|midBody|} \cdot W_{hip} \cdot 47\% \quad (2)$$

4) the location of the last thoracic vertebra, T_{12} (KP18) is computed as a point on the $midBody$ at a fraction of its length:

$$KP18 = KP17 + midBody \cdot 36\% \quad (3)$$

The numerical values used in these equations are based on the average vertebrae heights as reported in the literature [17] and on the normative segment dimensions reported in widely used anthropometric tables [5].

The resulting KPs are 19 expressed in pixel coordinates. To express them in metric coordinates, a conversion is performed by using the intrinsic parameters of the IR camera of the Kinect v2, which are the sensor's optical center along the X and Y coordinates C_x and C_y, and the sensor's focal length along the X and Y coordinates F_x, F_y. Therefore, to convert a point $P_{px} = (i, j)$ expressed in pixel coordinates to its corresponding point $P_m = (X, Y, Z)$ expressed in meters coordinates the formula is:

$$X = Z \cdot \frac{(i + k - C_x)}{F_x}$$
$$Y = Z \cdot \frac{(j + k - C_y)}{F_y} \quad (4)$$

given that the Z coordinate of P_m is known from the depth map. The correction parameter k is used to address distortions and misalignments that may happen during the color-depth registration procedure done internally by the Kinect v2, hence, in this case, is known and equal to 0.5 px.

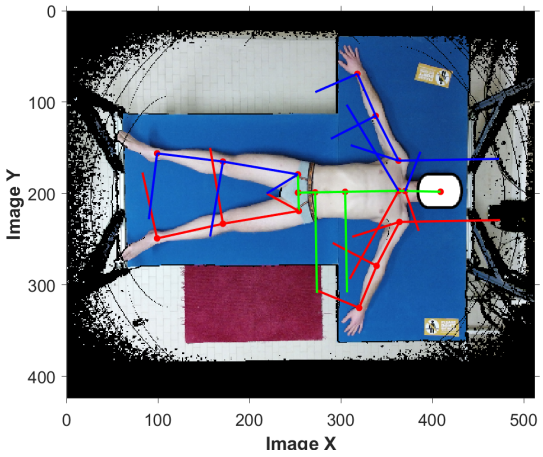

Fig. 3. Example of the vectors computed by the biomechanical model drawn on a color image of a subject. Red vectors refer to left KPs, blue vectors to right KPs, and green vectors to the trunk KPs.

E. Volume estimation algorithm

The volume estimation procedure is conducted following three steps: (i) body segments separation, (ii) body segments point cloud filling, (iii) Montecarlo volume computation.

1) Body segments separation: Since the subject's point cloud is centered in RF_{bed}, the separation of body segments point clouds can be easily done by projecting the subject's point cloud on the XY plane. Using the vectors of the biomechanical model, it is possible to build enclosing polygons (EP) around the segments and detect which points fall inside the EP. This process also acts as a further filtering step because the eventual background noise that may still be present in the cloud is discarded if it does not belong to the EPs. To compute the EPs it is sufficient to calculate the equation of orthogonal and parallel lines starting from both the vectors and the 19 KPs of the biomechanical model of the subject. For most BS the EP is determined by the intersection of 4 to 5 lines. However, special BS such as the shoulders (which is determined by 8 lines), the head, the hands, and the feet (which are all computed considering their proximal KPs and the corresponding vectors but do not have a distal KPs) are computed with an ad-hoc routine. The output of this step is a MATLAB structure in which each BS point cloud is stored

according to the corresponding EP. In Fig. 4 an example of this separation is shown using different colors.

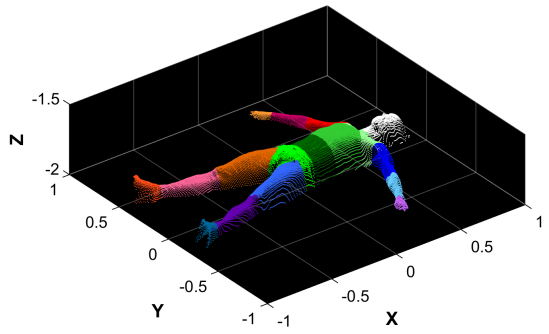

Fig. 4. Example of the BSs separation shown with different colors. Note that the point cloud of the head and feet is noisy due to the incorrect depth acquisition, corrected afterward.

2) Body segments point cloud filling: After the separation, some body segments may have wide gaps that interfere with the following elaboration, for example, the gap between the arm and the forearm in correspondence of the elbow KP. Moreover, by removing the bed from the cloud the bottom portion of the resulting body is empty and only the surface seen by the camera is present. Therefore, to address this issue two approaches are adopted:

- **bottom filling:** the bottom portion of each BS cloud is filled with artificial points created by copying the original BS cloud points and projecting them to the max Z coordinate corresponding to the position of the now removed bed.
- **gaps filling:** this step is only performed when the gaps originated by the BS separation are too wide or the shape of the BS has a particular geometry (i.e. shoulders and trunk body segments which have a pointy shape). In this case, artificial points at different Z coordinates are created starting from the XY coordinates of points belonging to the surface's edge.

For head and feet BSs the procedure is slightly different. In the case of the head, points laying at the max Z coordinate are treated as outliers to be removed in order to eliminate the effect of bad depth acquisition that happens due to the head's shape. Then, the bottom filling procedure is performed on the filtered cloud. In the case of the feet, depth acquisition fails because the shape of the feet points upwards but the IR ray is projected on the bed's surface (see Fig. 4). The result is a BS cloud that doesn't account for the plantar shape. Therefore, the idea is to separate the points belonging to the actual feet from those badly projected on the bed by using a KNN procedure with 3 centroids. The centroid closer to the max Z coordinate represents points that must be eliminated from the cloud. It is worth noting that feet BSs do not undergo any other filling process after this filtering.

3) Montecarlo volume computation: To estimate the volume of an object using the Montecarlo procedure as detailed in [18], the idea is to enclose the 3D object in a rectangular cuboid. Each size of the cuboid is computed considering the minimum and maximum corresponding size of the 3D object. The cuboid is then filled with $N >= 100000$ Montecarlo points. The volume of the object is therefore calculated as:

$$V_{object} = \frac{N_{object}}{N} \cdot V_{cuboid} \tag{5}$$

where V_{cuboid} is the volume of the cuboid (easily computed since it is of known size) and N_{object} corresponds to the number of Montecarlo points that falls inside the 3D object shape.

However, the procedure detailed in [18] to correctly compute N_{object} is extremely time-consuming. Therefore, in this work, we propose a faster approach leveraging alpha shapes. The alpha shape of a set of points is a definition of its shape in the 2D or 3D space. It is a generalization of the convex hull and a subgraph of the Delaunay triangulation; hence, the convex hull is just one type of alpha shape, and the full family of alpha shapes can be derived from the Delaunay triangulation of a given point set. The alpha parameter is defined as the value a, such that an edge of a disk of radius $1/a$ can be drawn between any two edge members of a set of points and still contain all the points [19]. The alpha shape of a set of points is computed by using the MATLAB function *alpaShape*. Then, the value of N_{object} is obtained by converting the alpha shape to a polyhedron and simply counting which Montecarlo points are inside it. However, to ensure that the computation is done properly, the BS point cloud should not have large gaps. It is worth noting that for each BS, the a parameter is set differently to account for the differences between shapes (i.e. the arm shape is very different from the trunk shape). Values used in this work were found experimentally and are: (i) 0.08 for the head, shoulders, pelvis, arm, shank, and foot BS, (ii) 0.05 for the forearm and hand BS, (iii) 0.15 for the trunk BS, (iv) 0.2 for the abdomen BS, and (v) 0.22 for the leg BS.

F. Mass estimation

For each body segment, a density value was assumed using data available from the literature [5]. For density not reported in the literature a fixed value was assumed as 1 g/cm^3. The mass of each segment was computed by multiplying this density value times the estimated volume.

III. Experiment

A. Protocol

Each subject is informed about the experiment and his/her rights according to the Helsinki declaration. The subject is then asked to undress, keeping only the underwear (and the brassiere for women), to remove unnecessary devices such as watches, necklaces, bracelets, glasses, and earrings, and to wear an elastic cap to prevent hair from being identified as a body segment. The experimental protocol itself is divided into two parts. The first part requires a trained staff member to measure the subject's body using a sartorial tape as a reference control. The manual measurements taken this way are:

- **arm, forearm, leg, shank:** proximal and distal circumferences O_p and O_d, segment's length $D_{segment}$
- **head:** circumference of the head O_{head} taken 1 cm higher than the ears, length L_{head} taken from $C7$ to the head tip
- **trunk and abdomen:** distance between the shoulders $D_{shoulders}$, circumference of the chest O_{chest} taken in correspondence of the nipples, circumference and width of the sternum $O_{sternum}$ and $W_{sternum}$, circumference and width in correspondence of $T10$ O_{T10} and W_{T10}, length of the trunk L_{trunk} taken from $C7$ to $T10$, length of the abdomen $L_{abdomen}$ taken from $T10$ to $L5$
- **pelvis:** distance between the two asi D_{asi}, circumference and width of the hips taken in correspondence of the asis O_{asi} and W_{asi}, width of the trochanters W_{troch}, distance from the asi to the trochanter $D_{asi-troch}$
- **hands:** width and length of the right hand W_{hand}, L_{hand}
- **feet:** width and length of the right foot W_{foot}, L_{foot}, circumference of the ankle O_{ankle}, height of the heel taken from the ankle to the ground H_{foot}

While the first part of the protocol is required only during the validation of the proposed method, the second part of the protocol is the actual measurement, and the only one to be actually performed to assess the subject's body segments' parameters. The second part requires the subject to lie on the bed for the 3D data acquisition. The posture must be the following: (i) head face-up near the edge of the structure, (ii) arms straightened near the bottom angles of the upper portion of the bed with an angle of around 60° between arms and chest, hands palms down, (iii) legs slightly apart at around shoulder's length, and (iv) feet orthogonal with respect to the bed, toes facing up.

During the volume acquisition procedure, the patient is asked to exhale all the air from the lungs to avoid detecting an over-expanded chest. The operator should count backward to inform the subject of the start of the acquisition. The patient should hold his breath until the end of the acquisition process, which takes about three seconds.

B. Experimental campaign

Data for the present study were collected from December 2022 to March 2023 at the University of Brescia. A total of 30 participants (18 males, 12 females, average age of 26 years old) were recruited. Inclusion criteria were age 18-79 years and the ability to give informed consent. Exclusion criteria were inability to lay down and still on the bed, uneasiness to undress in their underwear, and any condition affecting the body shape (i.e., amputations, pregnancy). Each subject signed a written informed consent before inclusion in the study detailing the experimental campaign. No personal data was stored except for those needed for the tests. The data collected was treated according to the Helsinki declaration.

IV. Results

Two different sets of body segments' parameters were obtained: masses and lengths. All segments' lengths were normalized by dividing the value obtained by the subject's height and then compared with the manual measurements taken by the expert operator in the first part of the protocol. Hands, feet, and the head were excluded from the comparison since the KPs of these segments do not coincide with their endpoints. Lengths comparison are here reported in Table 1 and in Fig. 5.

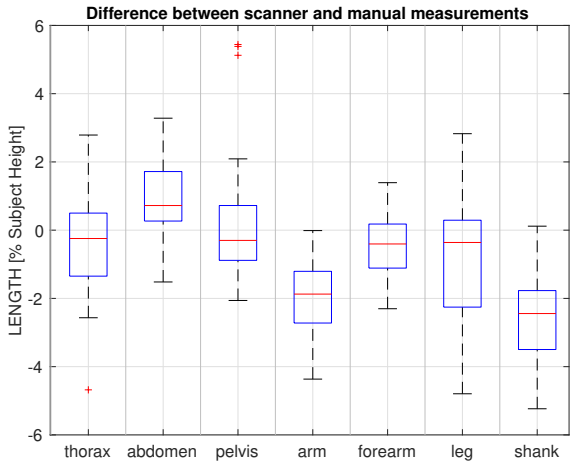

Fig. 5. Difference between segments' lengths as measured by the scanner and the same length measured manually by an expert operator. Values are normalized on the subject's height.

All segments' masses were normalized by dividing the value obtained by the subject's weight and then compared with the values reported in the literature by Dumas [5]. Masses comparisons are here reported in Table 1 and in 6. Since the population involved in this study differs from the population used to assess the values in [5] the difference between the two is reported here as an indication of the two approaches' differences and similarities and not as an indicator of an error in the measurements of volumes.

V. Discussion

The results reported in Fig. 5 show clearly that the scanner is able to identify correctly the endpoint of the segments within a 3% of the subject's height, making us confident that the separation into body segments starting from the image is accurate enough for most biomechanical research studies. Hands, feet, and head are missing from the length analysis, but being extreme segments this has a limited impact. The proposed 3D acquisition performs well and fast even if only one camera was adopted, however, in future developments a multi-Kinect set-up will be explored as well. The comparison of segments' masses reported in Fig. 6 gives mixed results: on one side it's clear that the median is close to the values assessed using anthropometric tables, on the other, it displays great variability in the differences between the two. This study involved adults, young adults, males, and females subjects. The variability of the population body segments is clearly visible by looking at the variance of the two main body

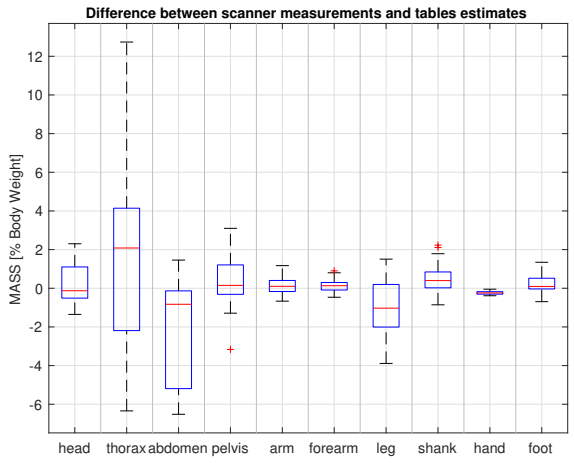

Fig. 6. Difference between segments' masses as measured by the scanner and the same mass estimated using anthropometric tables based on Dumas[5]. Values are normalized on the subject's weight.

TABLE I
COMPARISON OF SCANNER RESULTS WITH REFERENCE DATA

Segment	**difference between lengths scanner - manual meas. % of subject's height**		**difference between masses scanner - Dumas 2005 % of body weight**	
	mean	st.dev	mean	st.dev
$head$	n/a	n/a	1.0	1.4
$thorax$	-0.3	1.6	4.6	8.1
$abdomen$	0.9	1.0	-2.2	2.7
$pelvis$	0.3	2.0	2.0	2.8
arm_L	-1.8	1.2	0.3	0.4
arm_R	2.1	1.0	0.4	0.4
$forearm_L$	-0.1	0.9	0.2	0.3
$forearm_R$	-0.8	0.7	0.3	0.2
leg_L	-0.6	1.7	0.6	1.4
leg_R	-1.0	1.7	0.6	1.5
$shank_L$	-2.4	1.3	1.0	0.9
$shank_R$	-2.7	1.4	1.0	1.0
$hand_L$	n/a	n/a	-0.2	0.1
$hand_R$	n/a	n/a	-0.2	0.1
$foot_L$	n/a	n/a	0.3	0.5
$foot_R$	n/a	n/a	0.3	0.5

segments: the thorax (with a standard deviation of 8% of the body weight) and the abdomen (with a standard deviation of 3% of the body weight). Other possible sources of variability for the thorax and abdomen could be the subject respiratory phase, as the user was asked to exhale during the scan but no control over the air content was performed. Finally, the bed itself could play a role, since the supine position changes the spine curvature with respect to a standing pose, altering the proportion between the thoracic and lumbar segments of the back. Furthermore, the amount of tested subjects is still not enough to reach a satisfactory result since the collected dataset may be unbalanced. In further developments, motion-impaired patients will be tested as well to validate the robustness of the approach.

REFERENCES

[1] D. Thelen and F. Anderson, "Using computed muscle control to generate forward dynamic simulations of human walking from experimental data," *Journal of Biomechanics*, vol. 39, 2006.

[2] G. Rao, D. Amarantini, E. Berton, and D. Favier, "Influence of body segments' parameters estimation models on inverse dynamics solutions during gait," *J. Biomech.*, vol. 39, pp. 1531–1536, 2006.

[3] M. Damavandi, N. Farahpour, and P. Allard, "Determination of body segment masses and centers of mass using a force plate method in individuals of different morphology," *Medical Engineering and Physics*, vol. 31, no. 9, pp. 1187–1194, 2009.

[4] S. Pheasant and C. M. Haslegrave, *Bodyspace: Anthropometry, ergonomics and the design of work*. CRC press, 2005.

[5] R. Dumas, L. Cheze, and J. Verriest, "Adjustments to mcconville et al. and young et al. body segment inertial parameters," *J Biomech*, vol. 40, 2007.

[6] D. Winter, "Anthropometry," in *Biomechanics and Motor Control of Human Movement*. John Wiley I& Sons, Ltd, 2009, ch. 4, pp. 82–106, ISBN: 9780470549148.

[7] P. de Leva, "Adjustments to zatsiorsky-seluyanov's segment inertia parameters," *Journal of Biomechanics*, vol. 29, no. 9, pp. 1223–1230, 1996, ISSN: 0021-9290.

[8] E. Brolin, *Anthropometric diversity and consideration of human capabilities*. Chalmers University of Technology, 2016.

[9] J. L. Durkin and J. J. Dowling, "Analysis of body segment parameter differences between four human populations and the estimation errors of four popular mathematical models," *Journal of Biomechanical Engineering*, vol. 125, no. 4, pp. 515–522, 2003.

[10] C.-W. Tan, F. Coutts, and C. Bulley, "Measurement of lower limb volume: Agreement between the vertically oriented perometer and a tape measure method," *Physiotherapy*, vol. 99, no. 3, pp. 247–251, 2013.

[11] P. Dávila, E. Carrera, O. Jara, and H. Bassantes, "Design of a low cost 3d scanner for taking anthropometric measurements," in *International Conference on Applied Human Factors and Ergonomics*, Springer, 2019, pp. 971–978.

[12] S. Clarkson, J. Wheat, B. Heller, and S. Choppin, "Assessing the suitability of the microsoft kinect for calculating person specific body segment parameters," in *European Conference on Computer Vision*, Springer, 2014, pp. 372–385.

[13] C. Pfitzner, S. May, and A. Nüchter, "Body weight estimation for dose-finding and health monitoring of lying, standing and walking patients based on rgb-d data," *Sensors*, vol. 18, no. 5, p. 1311, 2018.

[14] K. Bartol, D. Bojanić, T. Petković, and T. Pribanic, "A review of body measurement using 3d scanning," *IEEE Access*, vol. PP, pp. 1–1, Apr. 2021.

[15] V. Bazarevsky, I. Grishchenko, K. Raveendran, T. Zhu, F. Zhang, and M. Grundmann, *Blazepose: On-device real-time body pose tracking*, 2020.

[16] E. Consortium. "Eurobench human model." (2020), [Online]. Available: https : / / github . com / aremazeilles / eurobench_ documentation (visited on 07/01/2022).

[17] M. E. Kunkel, A. Herkommer, M. Reinehr, T. M. Böckers, and H.-J. Wilke, "Morphometric analysis of the relationships between intervertebral disc and vertebral body heights: An anatomical and radiographic study of the human thoracic spine," *Journal of Anatomy*, vol. 219, no. 3, pp. 375–387, 2011.

[18] N. Covre, A. Luchetti, M. Lancini, S. Pasinetti, E. Bertolazzi, and M. De Cecco, "Monte carlo-based 3d surface point cloud volume estimation by exploding local cubes faces," *Acta IMEKO*, vol. 11, article 32, 2 Jun. 2022.

[19] H. Edelsbrunner, "Alpha shapes — a survey," 2009.